Computational Simulation and Analysis of Local Thermal Comfort and Indoor Air Quality in Space with Displacement Ventilation

Mohamad Kanaan
Mechanical Engineering Department, Faculty of Engineering, Beirut Arab University, P.O. Box 11-5020, Riad El Solh, Beirut, 1107-2809, Lebanon
m.kanaan@bau.edu.lb (corresponding author)

Semaan Amine
College of Engineering and Technology, American University of the Middle East, Egaila 54200, Kuwait
semaan.amine@aum.edu.kw

Eddie Gazo-Hanna
College of Engineering and Technology, American University of the Middle East, Egaila 54200, Kuwait
eddie-hanna@aum.edu.kw

Received: 27 May 2024 | Revised: 23 June 2024 | Accepted: 5 July 2024

 DOI: https://doi.org/10.48084/etasr.7948

ABSTRACT

Displacement ventilation has been known for its capacity to lower energy consumption and improve air quality, but it has major thermal comfort limitations. The aim of this paper is to optimize the DV supply conditions by using computational fluid dynamics modeling to achieve acceptable CO_2 concentration in the breathing layer at minimum energy cost while preventing local discomfort due to draft and air temperature difference between ankles and head. The results revealed that up to 44% energy savings can be achieved if the selection of supply conditions is optimized. The model can be put into practice to give recommendations on displacement ventilation preliminary design.

Keywords-displacement ventilation; CFD modeling; indoor air quality; local discomfort; energy consumption

I. INTRODUCTION

A successful Heating, Ventilation and Air-Conditioning (HVAC) system aims to provide both thermal comfort and acceptable air quality in indoor environments. However, designers must be concerned with the energy consumption issue and its negative impact on the environment. One of the air distribution systems that has been proven effective and energy efficient is Displacement Ventilation (DV). Its advantages are derived from the DV flow dynamics that divide the space vertically into two zones: the lower room that is clean and cool, and the upper room that is contaminated and hot. Consequently, better environmental quality is provided in the occupied zone while less energy is consumed as the system does not eventually cool the whole volume of the indoor air. The DV strategy consists of supplying conditioned air near the floor and extracting it at the ceiling level. However, supplying cool air on the floor level may result in local discomfort and excessive thermal stratification [1]. The DV air must be supplied at relatively low velocities (typically < 0.2 m/s) to reduce draft risk [2] and stratification must be controlled to avoid discomfort due to "warm head and cold feet." Furthermore, the supply air temperature must be higher than that of conventional air-conditioning systems, typically in the range from 18 to 22 [3, 4]. This provides an opportunity for reducing energy consumption but limits the applicability of DV systems to cooling loads no more than 40 W/m^2 [5]. When the cool air meets heat sources, it heats up and then displaces upward by natural convection. After that it carries the air contaminants to the upper room leaving the occupied zone fresh and clean [6].

The stratified DV airflow is primarily governed by the interaction of supply air with the thermal plumes rising above heat sources and in the vicinity of warm walls. An important controlling parameter of the DV flow is the stratification height at which the sum of rising plume flow rates equalizes the supply airflow rate. Above the stratification height, the airflow goes downward since the total volume of plumes exceeds the supply air volume. Another critical height is the plume terminal height at which the density gradients disappear in the rising air and the plume spreads horizontally. In this case a fully mixed zone starts to build up in the upper room.

Many researchers have investigated the Indoor Air Quality (IAQ) and thermal comfort in built environments conditioned with DV and reported important implications on the DV system design [7, 8]. IAQ refers to the air quality in terms of airborne pollutant concentration levels within and around buildings and structures. It is directly related to the well-being, comfort and health of the occupants. While developing design charts for DV systems integrated with chilled ceilings, authors in [9] indicated that IAQ is represented by the stratification height that must be above 1.2 m (sitting height), and that thermal comfort is represented by the room temperature gradient that should be less than 2.5 K/m. Authors in [10] modeled the transport of active particles in DV spaces. They reported that the stratification in particle concentration established by displacement ventilation is lowered as the particle diameter increases until reaching a critical diameter where the particle deposition onto surfaces overcomes the DV effect. Other studies [11, 12, 13] investigated the conjuncture of DV system with personalized ventilation to improve air quality and save energy. The use of personalized ventilation at flow rates ranging from 4 L/s to 10 L/s was reported to be able to improve the quality of inhaled air significantly in the breathing zone. Authors in [14] compared the performances of DV and mixing ventilation from the viewpoint of thermal comfort using validated Computational Fluid Dynamics (CFD) models. They concluded that through proper design, DV can maintain a thermal comfort environment at less energy cost. Authors in [15, 16] reported that a vertical temperature gradient from 4 ^{o}C to 5 ^{o}C slightly affected the local thermal comfort in DV applications. Another study [17], showed that seated occupants accepted up to 8 ^{o}C temperature difference between ankles and head over wide ranges of air speed, temperature, and turbulent intensity. Several studies have discussed the optimization of the design and operation of displacement ventilation systems [18]. However, none of them coupled the criteria of IAQ and local thermal comfort in addition to energy performance in the optimization work. The aim of this paper is to optimize the DV operational parameters to achieve both acceptable IAQ and local thermal comfort for better well-being and higher productivity of occupants while minimizing energy consumption.

II. METHODS

This study considers a hypothetical room served by a DV system and containing two occupant simulators and a point source of CO_2. A steady-state three-dimensional CFD model is developed using ANSYS Fluent, a commercial non-linear finite volume analysis software, to predict the velocity, temperature, and species concentration fields for different sets of parameters. Many studies concluded that CFD applications to indoor airflow simulation achieved considerable successes [19-23]. In fact, CFD can provide reasonably accurate predictions when correct governing equations, boundary conditions, and appropriate numerical schemes are carefully selected [24]. Several simulations were performed while varying the supply air flow rate, temperature, and velocity to find the best choice of supply conditions based on IAQ, local thermal comfort, and energy consumption.

A. Physical Model

The indoor space under study is a 2.5 m (W) × 2.8 m (L) × 2.5 m (H) displacement ventilated room that contains two cylindrical 100 W heat sources of 0.47 m diameter and 1.1 m height representing two seated occupants [12], as shown in Figure 1. A circular hole of 1 cm diameter positioned at a of 0.9 m height in the wall supplies 16.8 L/min of air at 32 °C with 4% in CO_2 volume representing the expiratory activity for two talking and breathing adult persons [25]. The lighting load is typical of 12 W/m^2. The walls of the room are adiabatic. The supply grill lower edge is at 20 cm above the floor.

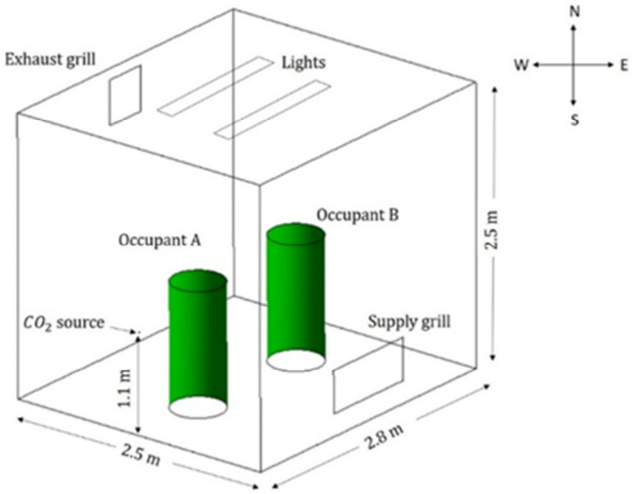

Fig. 1. Schematic of the simulated DV room.

B. Discretization and Meshing

The room's geometry is divided into 600,517 tetrahedral elements ensuring grid independency and the mesh quality is verified with a maximal cell skewness of 0.86. Mesh refinement was applied to openings and around heat sources to accurately capture the physics of high-gradient regions. The discretization of all governing equations was conducted using a second-order upwind scheme. This scheme achieves high-order accuracy at cell faces by employing a Taylor series expansion of the cell-centered solution around the cell centroid. The first order standard scheme was used for discretizing the pressure term. The velocity and pressure coupling in the Navier-Stokes equation was achieved using a simple algorithm. This algorithm creates an association between velocity and pressure corrections, guaranteeing mass conservation and streamlining the determination of the pressure field.

C. Computational Modeling

For steady-state three-dimensional incompressible turbulent flow, the Navier-Stokes equation is given by:

$$\frac{\partial(U_j U_i)}{\partial x_j} = -\frac{\partial P}{\rho \partial x_i} + \frac{\partial}{\partial x_j}\left(\nu \frac{\partial U_i}{\partial x_j} - \overline{u_i' u_j'}\right) + \frac{\rho - \rho_0}{\rho} g_i \quad (1)$$

To close the Navier-Stokes and Reynolds stress equations, the standard *k*-*ε* model was employed where one transport equation for turbulent kinetic energy, *k*, and another for turbulent dissipation rate, *ε*, where added to simulate turbulence and air recirculation. The standard *k-ε* model is known for its accuracy in predicting indoor flows and air pollutants dispersion [26-28] The energy model was activated and buoyancy was modeled using the Bossiness approximation for faster convergence [29]. Thermal radiation effects were included using the Surface-To-Surface (S2S) model which calculates the radiative heat exchange in an enclosure of gray-diffuse surfaces. The species transport model with an air-CO_2 mixture activated to solve the steady-state species transport problem represented by [30, 31]:

$$\frac{\partial}{\partial x_i}\left[U_i C - (D + D_t)\frac{\partial C}{\partial x_i}\right] = 0 \quad (2)$$

where D is the molecular diffusivity and D_t is the Eddy diffusivity. The generation term is treated as a boundary condition in the simulations.

The solution controls were set to default values and manipulated when solution manifested instability or divergence. The solution's consideration converged when the values of temperature and species concentration at room exhaust were stabilized, the scaled residuals reached 5×10^{-5} and the net heat and mass fluxes became less than 5% of the smallest flux in the computational domain.

D. Boundary Conditions

The boundary conditions used in the simulations are presented in Table I.

TABLE I. BOUNDARY CONDITIONS OF THE CFD SIMULATIONS

Boundary	Type	Details
DV supply grill	Velocity inlet	Velocity: 0.12 m/s, CO_2 molar fraction: 0.0004 (400 ppm in outdoor air), hydraulic diameter: 0.53 m, turbulent intensity: 5% [22].
Exhaust grill	Pressure outlet	Default values
Heated cylinder	No-slip	Heat flux: 56 W/m^2
CO2 source	Velocity inlet	Velocity: 1.78 m/s, temperature: 32 °C, CO_2 molar fraction: 0.04, hydraulic diameter: 0.01m.
Ceiling		Heat flux: 12 W/m^2
Room walls		Zero heat flux

E. IAQ Assessment Criteria

A breathing layer is defined in the CFD domain as being the horizontal fluid layer between the heights of 0.88 m and 1.2 m [32]. The evaluated air quality is based on the volume-averaged CO_2 concentration in the breathing layer. However, ASHRAE recommends that the indoor CO_2 concentration cannot be higher than 700 ppm above the outdoor air for achieving occupant satisfaction with human bio effluents/body odor levels [33], the maximal allowed value in this study was set to 700 ppm as a conservative approach to prevent any health issues or lack of productivity.

F. Local Discomfort Assessment Criteria

In order to evaluate local thermal comfort in the DV space, a microclimate was defined for each occupant simulator as a rectangular zone surrounding the cylinder at 20 cm from its sides and top. Seated occupants may feel local discomfort if the temperature gradient is sufficiently large. In the current study, the percentage of dissatisfied, $PD_{temp.diff}$, will be obtained by interpolation using the curve fit observed in Figure 2 that describes $PD_{temp.diff}$ versus ΔT_{a-h}, the vertical air temperature difference between ankles (0.1 m above the floor) and head (1.1 m above the floor).

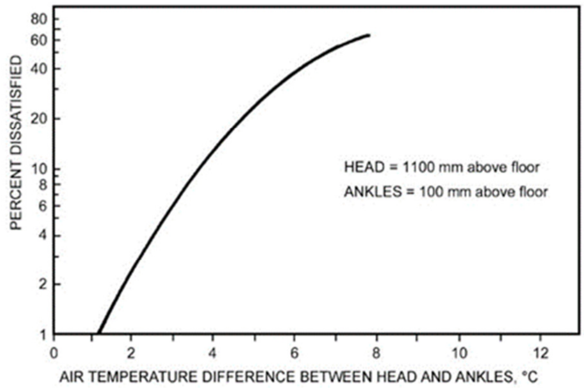

Fig. 2. Percentage of seated people dissatisfied due to the function of air temperature difference between head and ankles [34].

Another type of local discomfort is that occurring due to draft and can be predicted using Fanger's model [35]:

$$PD_{draft} = (34 - t_a)(V - 0.05)^{0.62} \times (0.37VTu + 3.14) \quad (3)$$

where PD_{draft} is the percentage of dissatisfied people by draft, t_a is the mean air temperature, V is the air speed, and T_u is the turbulent intensity percent. All air properties involved in the thermal comfort assessment are computed in the occupant's microclimate by the CFD code.

The local comfort's consideration is achieved when at least 80% of sedentary or slightly active people find the environment thermally acceptable [36]. In other words, both the percentages of dissatisfied people PD_{draft} and $PD_{temp.diff}$ must be maintained at or below 20% to prevent associated local discomfort.

G. Parametric Study and Energy Analysis

The purpose of the parametric study is to find the optimal set of supply conditions that minimize the energy consumption of the DV system while keeping acceptable IAQ and reducing to desired levels the local discomfort due to vertical thermal gradient and draft. In this endeavor, the DV chamber simulation parameters (different supply air flow rates, temperatures, and velocities) are listed in Table II. Initially, the supply flow rate was estimated by applying an energy balance to the room whose cooling load is about 40 W/m^2 of floor area and using a minimum supply temperature of 18 °C. The starting supply flow rate used in the first simulated case was about half of the estimated one based on the concept of partial volume cooling of the DV system. For higher energy efficiency, the supply flow rate was reduced until reaching the acceptable limit of CO_2 concentration at the breathing level and the supply temperature is increased until local discomfort occurs.

TABLE II. SUPPLY CONDITIONS FOR SIMULATION CASES

Case number	Supply airflow rate (m^3/s)	Supply air temperature (°C)	Supply grill area (m^2)	Supply air velocity (m/s)
1	0.042	18	0.34	0.12
2	0.042	20	0.34	0.12
3	0.033	18	0.34	0.095
4	0.025	18	0.34	0.07
5	0.025	18	0.25	0.1
6	0.025	20	0.34	0.07

The cooling coil power (kW) is calculated as follows:

$$\dot{Q} = \dot{m}_a(h_o - h_s) \quad (4)$$

where $\dot{m}_a$ is the supply air mass flow rate (kg/s) and h_o and h_s are the outdoor air and supply air enthalpies (kJ/kg), respectively. The outdoor design conditions were assumed to be those of Beirut for the cooling season: dry-bulb temperature T_{db} = 35 °C and wet-bulb temperature T_{wb} = 27 °C [37]. The sensible heat ratio of the room is typically 0.8.

III. METHODS

The CFD code is used to solve the conservation equations of mass, energy, and momentum to predict the three-dimensional patterns of fluid and heat flows. The most important feature of a successful DV simulation is to capture the dynamics of the DV flow that result from the interaction of the supply air with thermal plumes rising above heat sources and exhalation flows from occupants. Stratification height that divides the DV spaces into two zones of different fluid motion patterns must be established as well as associated thermal and species concentration stratification in the indoor air. This section presents the predicted velocity, temperature, and species concentrations fields in the simulated space.

A. Temperature Distribution

The indoor thermal fields on a vertical sampling plane are presented in Figure 3.

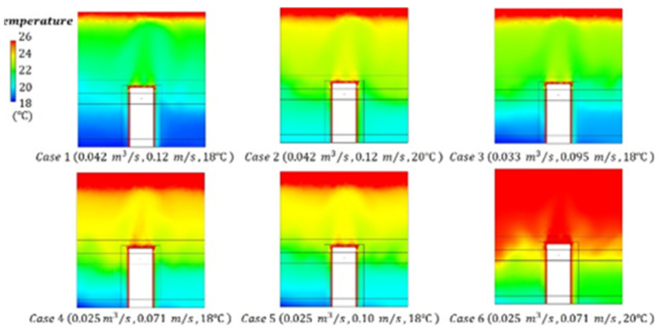

Fig. 3. Contour plots of thermal fields for all simulation cases.

The highest temperature values were obtained for the lowest ventilation rate and especially when DV air is supplied at higher temperature of 20°C (case 6). A lower cool zone and an upper warm zone can be identified in the temperature contour plots for all cases. However, the thermal stratification reduces with increasing supply flow rate and the system will behave like mixing if the supply flow rate is not controlled appropriately. It is noticeable that the stratification height that separates the two zones decreases with the supply flow rate since the total thermal plumes volume equalizes the supply air volume nearer to floor level. Also, the strength of stratification decreases as the supply temperature increases due to smaller thermal gradients in the room.

B. Airflow Distribution

Figure 4 shows the air velocity vector plots in the simulated DV room on a vertical sampling for all cases. The buoyancy-driven flow is well predicted where the thermal plume above heat sources is captured and the air recirculation above the stratification level is well predicted.

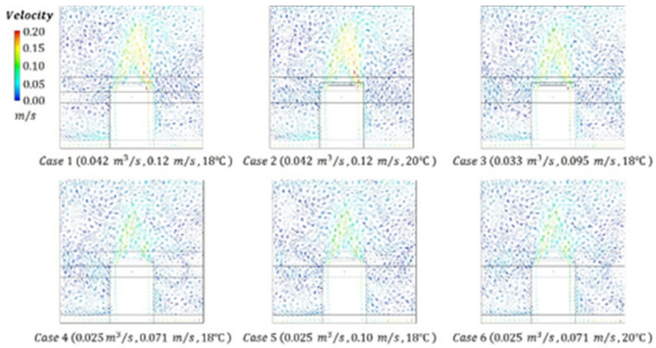

Fig. 4. Air velocity vector plots for all simulation cases.

As the supply flow rate decreases, air recirculation occurs at lower heights in the DV room since the stratification level gets lower. In fact, the system's behavior approaches the underfloor air distribution system as the supply velocity decreases and then air recirculation may occur in the lower zone and a piston flow may characterize the upper room. [38] On the other hand, the plume flow rate increases with the supply temperature due to the lower thermal gradient in the room since the two quantities are inversely proportional for stratified environments [39]. The supply air velocity does not seem to have any significant effect on the overall airflow patterns.

C. CO_2 Distribution

The contour plots of CO_2 concentration fields for all simulated cases are shown in Figure 5.

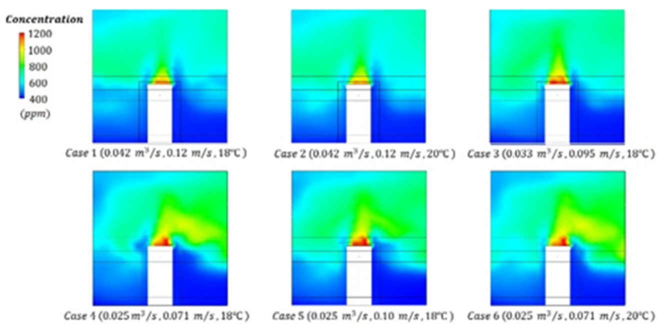

Fig. 5. Contour plots of CO_2 concentration fields for all simulation cases.

It is noticeable that the volume of the lower clean zone decreases with the supply flow rate due to the lowering of stratification height. Indoor concentration reaches higher levels for lower ventilation rates since less fresh air is introduced to the space. The CO_2 concentration at the room exhaust increased from 860 ppm to 989 ppm as the supply flow rate was reduced from 0.042 m^3/s to 0.025 m^3/s. The use of supply flow rates lower than 0.025 m^3/s will result in unacceptable IAQ since the average concentration in the breathing zone will exceed the standard limit of 700 ppm. CFD predictions showed that supply air velocity and temperature have negligible effect on the species distribution when the supply flow rate remains unchanged, which is consistent with the findings in [7].

D. Optimal DV Operational Parameters

It is of great interest to optimize the selection of DV supply conditions to meet the IAQ and concerned local comfort criteria while minimizing energy consumption. The predicted values of volume-averaged CO_2 concentration in the breathing layer, denoted $C_{avg,bz}$, for all simulated cases are shown in Table III. The values of all parameters needed for assessing and identifying local discomfort for the two occupants are presented in Tables IV and V. All listed values were computed within the occupants' microclimates.

TABLE III. VOLUME-AVERAGE CONCENTRATION IN THE BREATHING LAYER FOR ALL SIMULATION CASES

	Case 1	**Case 2**	**Case 3**	**Case 4**	**Case 5**	**Case 6**
$C_{avg,bz}$ (ppm)	615	613	651	697	692	700

TABLE IV. LOCAL DISCOMFORT PARAMETERS FOR OCCUPANT A

Case number	**ΔT_{a-h} (°C)**	**$PD_{temp.\,diff}$ (%)**	**t_a (°C)**	**V (m/s)**	**Tu (%)**	**PD_{draft} (%)**
1	2.8	3.6	20.1	0.32	8.94	25.8
2	2.72	5.4	22.12	0.31	9.27	21.66
3	3.4	8	20.8	0.25	10.08	20.22
4	4.35	18	22	0.23	10.4	17
5	4.27	17.5	21.8	0.22	10.5	16.47
6	4.4	19	24	0.23	10.53	14

TABLE V. LOCAL DISCOMFORT PARAMETERS FOR OCCUPANT B

Case number	**ΔT_{a-h} (°C)**	**$PD_{temp.\,diff}$ (%)**	**t_a (°C)**	**V (m/s)**	**Tu (%)**	**PD_{draft} (%)**
1	2.85	3.7	20.1	0.33	8.83	26.23
2	2.76	5.5	22.08	0.32	8.77	22.11
3	3.45	8.2	20.8	0.26	10.15	20.25
4	4.18	16.4	21.9	0.21	10.47	15.65
5	4.18	16.4	21.8	0.216	10.55	15.96
6	4.32	17.8	24	0.218	10.55	13.22

The results show that for cases 1, 2, and 3, the DV system can provide good IAQ but fails to achieve local thermal comfort with PD_{draft} > 20%. For cases 4, 5, and 6, the levels of local discomfort due to both draft and air temperature difference between ankles and head are acceptable with $PD_{temp.\,diff}$ < 20% and PD_{draft} < 20% and IAQ is acceptable as well. However, the DV system exhibits the lowest values of $PD_{temp,diff}$ and PD_{draft} and the highest energy efficiency (lowest supply air flow rate and highest supply temperature) in case 6, which makes it the optimal case. The judgment of IAQ and local comfort along with energy consumption for all cases are summarized in Table VI showing that moving from case 1 to optimal case 6, energy savings of up to 44% can be achieved on the system.

TABLE VI. SUMMARY OF PARAMETRIC STUDY RESULTS

Case number	**Acceptable IAQ**	**Local comfort for occupant A**	**Local comfort for occupant B**	**Cooling coil power in kW**
1	Yes	No	No	2.26
2	Yes	No	No	2.12
3	Yes	No	No	1.78
4	Yes	Yes	Yes	1.34
5	Yes	Yes	Yes	1.34
6	Yes	Yes	Yes	1.26

IV. CONCLUSION

A steady-state three-dimensional CFD model was developed to predict the airflow, temperature, and CO_2 concentration distributions in a displacement ventilated room. The CFD model used in a parametric study where the produced predictions were used to evaluate air quality in the breathing layer and local discomfort due to draft and air temperature difference between ankles and head in the vicinity of occupants for different cases. The simulation parameters were the supply air flow rate, temperature, and velocity. The results of the parametric study were used to optimize the selection of the DV parameters for acceptable IAQ and local comfort at minimum energy cost. The following conclusions can be drawn:

- Results showed that up to 44% energy savings can be achieved when moving from the worst case (case 1) to the optimal case (case 6) while improving the indoor environmental quality in the DV space.
- The findings of this study can be used to make few recommendations for preliminary design and optimization of similar ventilation projects.

REFERENCES

[1] K. W. D. Cheong, W. J. Yu, S. C. Sekhar, K. W. Tham, and R. Kosonen, "Local thermal sensation and comfort study in a field environment chamber served by displacement ventilation system in the tropics," *Building and Environment,* vol. 42, no. 2, pp. 525–533, Feb. 2007, https://doi.org/10.1016/j.buildenv.2005.09.008.

[2] Y. Li, M. Sandberg, and L. Fuchs, "Effects of thermal radiation on airflow with displacement ventilation: an experimental investigation," *Energy and Buildings*, vol. 19, no. 4, pp. 263–274, Jan. 1993, https://doi.org/10.1016/0378-7788(93)90011-I.

[3] N. Lastovets, R. Kosonen, P. Mustakallio, J. Jokisalo, and A. Li, "Modelling of room air temperature profile with displacement ventilation," *International Journal of Ventilation*, vol. 19, pp. 1–15, Mar. 2019, https://doi.org/10.1080/14733315.2019.1579486.

[4] Y. Kang, Y. Wang, and K. Zhong, "Effects of supply air temperature and inlet location on particle dispersion in displacement ventilation rooms," *Particuology*, vol. 9, no. 6, pp. 619–625, Dec. 2011, https://doi.org/10.1016/j.partic.2010.05.018.

[5] X. Yuan, Q. Chen, and L. Glicksman, "A critical review of displacement ventilation," ASHRAE Transactions, vol. 4101, pp. 78–90, Jan. 2001.

[6] C. Habchi, K. Ghali, and N. Ghaddar, "Comparison of Removal Effectiveness of Mixed versus Displacement Ventilation during

Vacuuming Session," *Renewable Energy and Power Quality Journal*, vol. 18, pp. 437–442, Jun. 2020, https://doi.org/10.24084/repqj18.371.

[7] M. Kanaan, N. Ghaddar, and K. Ghali, "Simplified Model of Contaminant Dispersion in Rooms Conditioned by Chilled-Ceiling Displacement Ventilation System," *HVAC&R Research*, vol. 16, pp. 765–783, Nov. 2010, https://doi.org/10.1080/10789669.2010.10390933.

[8] R. Cermak, A. Melikov, L. Forejt, and O. Kovar, "Performance of Personalized Ventilation in Conjunction with Mixing and Displacement Ventilation," *HVAC&R Research*, vol. 12, pp. 295–311, Apr. 2006, https://doi.org/10.1080/10789669.2006.10391180.

[9] N. Ghaddar, K. Ghali, R. Saadeh, and A. Keblawi, "Design charts for combined chilled ceiling displacement ventilation system," *ASHRAE Transactions*, vol. 143, pp. 574–587, Jan. 2008.

[10] C. Habchi, K. Ghali, and N. Ghaddar, "A simplified mathematical model for predicting cross contamination in displacement ventilation air-conditioned spaces," *Journal of Aerosol Science*, vol. 76, pp. 72–86, Oct. 2014, https://doi.org/10.1016/j.jaerosci.2014.05.009.

[11] M. Kanaan, N. Ghaddar, and K. Ghali, "Quality of Inhaled Air in Displacement Ventilation Systems Assisted by Personalized Ventilation," *HVAC&R Research*, vol. 18, May 2012, https://doi.org/10.1080/10789669.2012.649882.

[12] A. Makhoul, K. Ghali, and N. Ghaddar, "A simplified combined displacement and personalized ventilation model," *Hvac&r Research*, vol. 18, pp. 737–749, Aug. 2012, https://doi.org/10.1080/10789669.2011.605510.

[13] K. W. D. Cheong and S. Huang, "Performance evaluation of personalized ventilation system with two types of air terminal devices coupled with displacement ventilation in a mock-up office," *HVAC&R Research*, vol. 19, pp. 974–985, Nov. 2013, https://doi.org/10.1080/10789669.2013.838439.

[14] Z. Lin, T. T. Chow, K. F. Fong, Q. Wang, and Y. Li, "Comparison of performances of displacement and mixing ventilations. Part I: thermal comfort," *International Journal of Refrigeration,* vol. 28, no. 2, pp. 276–287, Mar. 2005, https://doi.org/10.1016/j.ijrefrig.2004.04.005.

[15] D. P. Wvon and M. Sandberg, "Discomfort due to Vertical Thermal Gradients," Indoor Air, vol. 6, no. 1, pp. 48–54, 1996, https://doi.org/10.1111/j.1600-0668.1996.t01-3-00006.x.

[16] W. J. Yu, K. W. D. Cheong, K. W. Tham, S. C. Sekhar, and R. Kosonen, "Thermal effect of temperature gradient in a field environment chamber served by displacement ventilation system in the tropics," *Building and Environment*, vol. 42, no. 1, pp. 516–524, Jan. 2007, https://doi.org/10.1016/j.buildenv.2005.09.003.

[17] S. Liu, S. Schiavon, A. Kabanshi, and W. W. Nazaroff, "Predicted percentage dissatisfied with ankle draft," *Indoor Air*, vol. 27, no. 4, pp. 852–862, 2017, https://doi.org/10.1111/ina.12364.

[18] M. Mossolly, K. Ghali, N. Ghaddar, and L. Jensen, "Optimized operation of combined chilled ceiling displacement ventilation system using genetic algorithm," *ASHRAE Transactions*, vol. 114, no. 2, pp. 541–555, Jul. 2008.

[19] A. Askari, M. Mahdavinejad, and M. Ansari, "Investigation of displacement ventilation performance under various room configurations using computational fluid dynamics simulation," *Building Services Engineering Research and Technology*, vol. 43, no. 5, pp. 627–643, Sep. 2022, https://doi.org/10.1177/01436244221097312.

[20] M. Kanaan, N. Ghaddar, K. Ghali, and G. Araj, "Upper room UVGI effectiveness with dispersed pathogens at different droplet sizes in spaces conditioned by chilled ceiling and mixed displacement ventilation system," *Building and Environment*, vol. 87, pp. 117–128, May 2015, https://doi.org/10.1016/j.buildenv.2015.01.029.

[21] E. Alizadeh, A. Maleki, and A. Mohamadi, "An Investigation of the Effect of Ventilation Inlet and Outlet Arrangement on Heat Concentration in a Ship Engine Room," *Engineering, Technology & Applied Science Research*, vol. 7, pp. 1996–2004, Oct. 2017, https://doi.org/10.48084/etasr.1288.

[22] F. Nasri, "Numerical Simulation of a Efficient Solar-Powered Ventilation System," *Engineering, Technology & Applied Science Research*, vol. 13, no. 4, pp. 11459–11465, Aug. 2023, https://doi.org/10.48084/etasr.6038.

[23] S. Alimi, R. Nciri, F. Nasri, Y. A. Rothan, and C. Ali, "Performance investigation of an original hybrid solar façade system used for HDH desalination and building natural ventilation," *Journal of Building Engineering*, vol. 42, pp. 102515, Oct. 2021, https://doi.org/10.1016/j.jobe.2021.102515.

[24] Y. Li and P. V. Nielsen, "CFD and ventilation research," *Indoor Air*, vol. 21, no. 6, pp. 442–453, 2011, https://doi.org/10.1111/j.1600-0668.2011.00723.x.

[25] C. Habchi, K. Ghali, N. Ghaddar, W. Chakroun, and S. Alotaibi, "Ceiling personalized ventilation combined with desk fans for reduced direct and indirect cross-contamination and efficient use of office space," *Energy Conversion and Management*, vol. 111, pp. 158–173, Mar. 2016, https://doi.org/10.1016/j.enconman.2015.12.067.

[26] A. J. Gadgil, C. Lobscheid, M. O. Abadie, and E. U. Finlayson, "Indoor pollutant mixing time in an isothermal closed room: an investigation using CFD," *Atmospheric Environment*, vol. 37, no. 39, pp. 5577–5586, Dec. 2003, https://doi.org/10.1016/j.atmosenv.2003.09.032.

[27] M. P. Wan and C. Y. Chao, "Numerical and experimental study of velocity and temperature characteristics in a ventilated enclosure with underfloor ventilation systems," *Indoor Air*, vol. 15, no. 5, pp. 342–355, Oct. 2005, https://doi.org/10.1111/j.1600-0668.2005.00378.x.

[28] Z. Hu, L. Wang, Y. Lu, and M. Yang, "Numerical Simulation of Airliner Cabin Environment based on Various Inlet Angles," *Journal of Engineering Science and Technology Review*, vol. 7, pp. 115–120, Jul. 2014, https://doi.org/10.25103/jestr.073.19.

[29] J. Lau and J. L. Niu, "Measurement and CFD Simulation of the Temperature Stratification in an Atrium Using a Floor Level Air Supply Method," *Indoor and Built Environment*, vol. 12, no. 4, pp. 265–280, Aug. 2003, https://doi.org/10.1177/1420326X03035917.

[30] Z. Zhang and Q. Chen, "Comparison of the Eulerian and Lagrangian methods for predicting particle transport in enclosed spaces," *Atmospheric Environment*, vol. 41, no. 25, pp. 5236–5248, Aug. 2007, https://doi.org/10.1016/j.atmosenv.2006.05.086.

[31] B. Zhao, Z. Zhang, X. Li, and D. Huang, "Comparison of diffusion characteristics of aerosol particles in different ventilated rooms by numerical method," *ASHRAE Transactions*, vol. 110, pp. 88–95, Jan. 2004.

[32] M. Kanaan, N. Ghaddar, and K. Ghali, "Localized air-conditioning with upper-room UVGI to reduce airborne bacteria cross-infection," *Building Simulation*, vol. 9, no. 1, pp. 63–74, Feb. 2016, https://doi.org/10.1007/s12273-015-0250-7.

[33] M. Falih, *Ventilation for Acceptable Indoor Air Quality.* 2020.

[34] A. S. of H. Incorporated Refrigerating &. Air Conditioning Engineers, *ASHRAE Fundamentals Handbook 2001*. American Society of Heating, Refrigerating & Air Conditioning Engineers, Incorporated, 2001.

[35] P. O. Fanger, A. K. Melikov, H. Hanzawa, and J. Ring, "Turbulence and draft.," Jan. 1989, Accessed: Jul. 25, 2024. [Online]. Available: https://www.aivc.org/resource/turbulence-and-draft.

[36] *Thermal environmental conditions for human occupancy*. Atlanta, GA, USA: American Society of Heating, Refrigerating, and Air-Conditioning Engineers, 1992.

[37] H. Mohsen, R. Raslan, and I. El-Bastawissi, "The impact of changes in beirut urban patterns on the microclimate: a review of urban policy and building regulations," *Architecture and Planning Journal*, vol. 25, Jan. 2020, https://doi.org/10.54729/2789-8547.1001.

[38] H. Ito and N. Nakahara, "Simplified calculation model of room air temperature profile in under-floor air-conditioning system."

[39] H. D. Goodfellow and E. Tahti, *Industrial Ventilation Design Guidebook*. Academic Press, 2001.